

**NEAR SURFACE GEOPHYSICAL IMAGING FOR  
SHALLOW GROUNDWATER FLOW  
EVALUATION USING ELECTRICAL  
RESISTIVITY AND SELF-POTENTIAL  
METHODS**

**ADEEKO TAJUDEEN OLUGBENGA**

**UNIVERSITI SAINS MALAYSIA**

**2020**

**NEAR SURFACE GEOPHYSICAL IMAGING FOR  
SHALLOW GROUNDWATER FLOW  
EVALUATION USING ELECTRICAL  
RESISTIVITY AND SELF-POTENTIAL  
METHODS**

by

**ADEEKO TAJUDEEN OLUGBENGA**

**Thesis submitted in fulfilment of the requirements  
for the degree of  
Doctor of Philosophy**

**July 2020**

## ACKNOWLEDGEMENT

I am forever grateful to God the father, the Son, and the Holy Spirit, for inspiring and protecting me through this period of my course, and for the gift of life and numerous blessing upon my life. I am profoundly thankful to my supervisor Dr. Nordiana Binti Mohd Muztaza, who with her unique research competence, selfless devotion, thoughtful guidance, inspirational thoughts, wonderful patience and above all parent like direction, behaviour and affection motivated me to pursue this work. I also thank my co-supervisor Dr. Nur Azwin Binti Ismail for her support and advice. A lot of thank to my colleagues especially, Taquiuddin Zakaria, Afiq Saharudin, Nabila Sulaiman, Umi Maslinda, Nordiana Ahmad, Nur Amalina Anuar, Nurina Ismail, and the laboratory assistants, Mr. Yaakub Othman, Mr. Shahil Ahmad Khosaini, Mr. Zulkeflee Ismail, and Mr. Azmi Abdullah for their support during the data acquisitions.

My immense gratitude goes to my dearest unique queen, Lilian Adeeko and my pretty daughter, Esther Adeeko and my handsome son, Enoch Adeeko for their sacrifices of love, care, understanding, prayer, and support throughout my stay in this citadel of higher learning. My appreciation goes to my father Late Mr. L.A. Adeeko, my mother Mrs. E.F. Adeeko, and my sisters, brothers and the entire family and all my spiritual leaders. Also thank Universiti Sains Malaysia for the opportunity given to me through the Graduate Research Assistant within the project plan FRGS entitled development of 2-D linear inversion algorithm from geophysical approach for soil or rock characteristics (203/PFIZIK/6711663) and RUI entitled integrated geophysical characterization of geothermal exploration and strategy for a sustainable use of geothermal resources (1001/PFIZIK/8011110). My apology goes to all those whose names could not be mention here due to space factor; I cherish their support with silent

gratitude. I lack appropriate words to express my gratitude and indebtedness to you all but pray the Almighty God to reward each, and every one of you abundantly Amen. Finally, I would express thank to my employer, University of Abuja, Nigeria for granting me study leave and financial assistance in pursuit of my PhD degree through the Academic Staff Training and Development (ASTD).

## TABLE OF CONTENTS

<b>ACKNOWLEDGEMENT .....</b>	<b>ii</b>
<b>TABLE OF CONTENTS.....</b>	<b>iv</b>
<b>LIST OF TABLES .....</b>	<b>viii</b>
<b>LIST OF FIGURES .....</b>	<b>x</b>
<b>LIST OF SYMBOLS .....</b>	<b>xiv</b>
<b>LIST OF ABBREVIATIONS .....</b>	<b>xv</b>
<b>LIST OF APPENDICES.....</b>	<b>xvii</b>
<b>ABSTRAK.....</b>	<b>xviii</b>
<b>ABSTRACT .....</b>	<b>xx</b>
<b>CHAPTER 1 INTRODUCTION.....</b>	<b>1</b>
1.1 Background of the study.....	1
1.2 Problem Statements.....	3
1.3 Objectives .....	4
1.4 Significant and Novelty of the study .....	4
1.5 Thesis layout .....	5
<b>CHAPTER 2 LITERATURE REVIEW .....</b>	<b>7</b>
2.1 Introduction.....	7
2.2 2-D Resistivity .....	10
2.3 Self-Potential Method (SP).....	12
2.4 Soil Hand Auger.....	13
2.4.1 Sieve Analysis and Grain-Size Distributions (GSDs).....	14
2.5 Previous Work.....	15
2.5.1 Granitic/coastal grain.....	15
2.6 Chapter summary .....	24

<b>CHAPTER 3</b>	<b>METHODOLOGY.....</b>	<b>26</b>
3.1	Introduction.....	26
3.2	Study Area .....	28
3.2.1	Geology of Penang and study area.....	29
3.2.1(a)	Archaeology Gallery Site one.....	30
3.2.1(b)	Perpustakaan Hamzah Sendut (PHS) 2 Site two .....	31
3.2.2	Geology of Kedah and study area.....	32
3.2.3	Geology of Kelantan and Study area .....	34
3.2.4	Geology of Kluang District Southern Peninsular Malaysia (Confidential).....	36
3.3	Data Acquisitions (Stage one).....	37
3.3.1	2-D Resistivity .....	37
3.3.2	Self-potential.....	38
3.4	Program Development.....	39
3.4.1	SortD program.....	42
3.4.2	SortD characteristics .....	43
3.4.3	SortD Code .....	46
3.5	Soil sample.....	46
3.5.1	Soil hand auger .....	46
3.5.2	Sieve Analysis and Grain-Size Distributions (GSDs).....	48
3.5.3	Calculation and expression of results.....	50
3.6	Chapter summary .....	52
<b>CHAPTER 4</b>	<b>RESULTS AND DISCUSSIONS.....</b>	<b>54</b>
4.1	Introduction.....	54
4.2	Results of all the study areas.....	55
4.2.1	Archaeology Gallery site one (USM) Penang .....	55
4.2.1(a)	2-D resistivity .....	55
4.2.1(b)	Self-potential.....	58

4.2.1(c)	Integration of 2-D resistivity and self-potential.....	60
4.2.1(d)	Sieving analysis and grain size distribution .....	62
4.2.1(e)	Slice by slice for 2-D resistivity and self-potential.....	69
4.2.2	Perpustakaan Hamzah Sendut (PHS) Site two (USM) Penang .....	75
4.2.2(a)	2-D resistivity .....	75
4.2.2(b)	Self-potential.....	77
4.2.2(c)	Integration of 2-D resistivity and self-potential.....	81
4.2.2(d)	Sieving analysis and grain size distribution .....	83
4.2.2(e)	Slice by slice for 2-D resistivity and self-potential.....	85
4.2.3	Sungai Batu, Kedah.....	89
4.2.3(a)	2-D resistivity .....	90
4.2.3(b)	Self-potential.....	92
4.2.3(c)	Integration of 2-D resistivity and self-potential.....	95
4.2.3(d)	Sieving analysis and grain size distribution .....	96
4.2.3(e)	Slice by slice for 2-D resistivity and self-potential.....	103
4.2.4	Lojing, Kelantan .....	107
4.2.4(a)	2-D resistivity .....	108
4.2.4(b)	Self-potential.....	111
4.2.4(c)	Integration of 2-D resistivity and self-potential.....	114
4.2.4(d)	Sieving analysis and grain size distribution .....	116
4.2.5	Kluang District of Southern Peninsular Malaysia (Confidential).....	121
4.2.5(a)	2-D resistivity .....	122
4.2.5(b)	Self-potential.....	123
4.2.5(c)	Integration of 2-D resistivity and self-potential.....	125
4.3	Summary and characterization of all the study areas .....	127
4.4	Chapter summary .....	129

<b>CHAPTER 5</b>	<b>CONCLUSION AND RECOMMENDATIONS .....</b>	<b>131</b>
5.1	Conclusion .....	131
5.2	Recommendations .....	132
<b>REFERENCES</b>	<b>.....</b>	<b>133</b>
<b>APPENDICES</b>		
<b>LIST OF PUBLICATIONS</b>		



## LIST OF TABLES

		<b>Page</b>
Table 2.1	Summary of the previous works.....	24
Table 3.1	Classification of soil type with their diameter.....	49
Table 3.2	Unconsolidated Sedimentary Materials (Ritzema, 2006) .....	52
Table 4.1	Borehole data (BH1) with the corresponding resistivity values at Archaeology gallery .....	57
Table 4.2	Summary results of dry soil sieving analysis for AS1 at distance 35 m at depth of 0.5 m at Archaeology gallery .....	63
Table 4.3	Summary of the grain size distribution and physical parameters for AS1, AS2, AS3 at Archaeology gallery .....	74
Table 4.4	Soil profile at Archaeology gallery USM.....	75
Table 4.5	Summary results of dry soil sieving analysis for PS1 at distance 14 m at depth of 0.5 m at Perpustakaan Hamzah Sendut (PHS 2)....	84
Table 4.6	Summary of the grain size distribution and physical parameters for PS1, PS2, & PS3 at PHS 2.....	89
Table 4.7	Soil profile at Perpustakaan Hamzah Sendut 2 (PHS).....	89
Table 4.8	Borehole data (BH10) with the corresponding resistivity values at Sungai Batu.....	92
Table 4.9	Summary results of dry soil sieving analysis for SS1 at distance 2.5 m at depth of 0.5 m at Sungai batu .....	97
Table 4.10	Summary of the grain size distribution and interpretation for SS1, SS1, SS3 at Sungai batu.....	107
Table 4.11	Soil profile at Sungai Batu.....	108
Table 4.12	Borehole data (BH1) with the corresponding resistivity values at Lojing.....	111
Table 4.13	Summary results of dry soil sieving analysis for LS1 at distance 35 m at depth of 0.5 m at Lojing .....	117
Table 4.14	Summary of the grain size distribution and interpretation for LS1, LS2, LS3 at Lojing.....	121

Table 4.15	Soil profile at Lojing Kelantan.....	121
Table 4.16	Summary of geophysical methods, geotechnical analysis, and soil description .....	129

## LIST OF FIGURES

		<b>Page</b>
Figure 2.1	Water cycle or hydrological cycle .....	8
Figure 2.2	Basic concept of electrical resistivity measurement.....	11
Figure 2.3	Simplified model of the origin of self-potential anomaly of an ore body. The operation based on differences in oxidation potential above and below the water table.....	13
Figure 3.1	Flow chart of the research methodology .....	27
Figure 3.2	Location of the study areas in Peninsular Malaysia .....	28
Figure 3.3	Geological map of Penang and Study area (modified after Mineral and Geoscience Department Malaysia, 2018).....	29
Figure 3.4	Study area show the survey lines in Archaeology Gallery (google earth, 2018).....	30
Figure 3.5	Study area show the survey lines in PHS 2 (google earth, 2018).....	32
Figure 3.6	Geological map of Kedah and Study area (modified after Mineral and Geoscience Department Malaysia, 2018).....	33
Figure 3.7	Study area show the survey lines in Sungai Batu (google earth, 2018) .....	34
Figure 3.8	Geological map of Kelantan and Study area (modified after Mineral and Geoscience Department Malaysia, 2018).....	35
Figure 3.9	Study area show the survey lines in Lojing (google earth, 2018) .....	36
Figure 3.10	Study area show the survey lines in Kluang District Southern Peninsular Malaysia.....	37
Figure 3.11	Equipment for 2-D resistivity method .....	38
Figure 3.12	Equipment for self-potential method .....	39
Figure 3.13	2-D resistivity raw data from notepad .....	40
Figure 3.14	2-D resistivity raw data in excel.....	40
Figure 3.15	2-D resistivity raw data with depth and distance (manual sorted data).....	41

Figure 3.16	Self-potential raw data in excel .....	41
Figure 3.17	Importance of sortD program.....	42
Figure 3.18	Data sorting flow chart (SortD).....	43
Figure 3.19	SortD user interface .....	44
Figure 3.20	Import file of 2-D resistivity sheet.....	44
Figure 3.21	Results for 2-D resistivity data sorting (for 2m spacing).....	45
Figure 3.22	Import file of self-potential sheet .....	45
Figure 3.23	Result for 2-D resistivity data sorting (for 2m spacing) .....	46
Figure 3.24	Equipment and tool for soil hand auger .....	47
Figure 3.25	Shaker and sieves set BS410 and receiving pan with sample .....	50
Figure 4.1	2-D resistivity inversion model for AG1 to AG7 with x-distance (m), y-elevation (m) at Archaeology gallery.....	56
Figure 4.2	Self-potential contour map from AG1 to AG7 generated by horizontal subsurface flow at Archaeology gallery .....	58
Figure 4.3	3-D wireframe map shows the flow of water direction generated by horizontal subsurface flow Archaeology gallery .....	59
Figure 4.4	Magnitude of self-potential (SP) at Archaeology gallery.....	60
Figure 4.5	2-D resistivity inversion model and self-potential profile for AG1(a) to AG7(g) at Archaeology gallery .....	61
Figure 4.6	Grain size distribution curve at 0.5 m depth for AS1 at Archaeology Gallery.....	62
Figure 4.7	Slice by slice for 3m distance of 2-D resistivity and SP at different depth a) 2-D resistivity placing vertical b) self-potential and c) horizontal at Archaeology gallery.....	70
Figure 4.8	2-D resistivity inversion model for PH1 to PH5 with x-distance (m), y-depth (m) at PHS 2.....	77
Figure 4.9	Self-potential contour map from PH1 to PH5 generated by horizontal subsurface flow at PHS 2.....	78
Figure 4.10	Contour map shows the flow of water direction generated by horizontal subsurface flow at PHS 2.....	79
Figure 4.11	The subsidence found in PHS 2.....	80

Figure 4.12	Magnitude of self-potential (SP) at PHS 2.....	81
Figure 4.13	Integration of 2-D resistivity inversion model and self-potential profile for PH1(a) to PH5(e) at PHS 2.....	82
Figure 4.14	Grain size distribution curve at 0.5 m depth for PS1 at PHS 2 .....	83
Figure 4.15	Slice by slice for 2 m distance of 2-D resistivity and SP at different depth placing vertical a) 2-D resistivity b) self-potential and c) horizontal at PHS 2.....	86
Figure 4.16	2-D resistivity inversion model for SB1 to SB4 with x-distance (m), y-depth (m) at Sungai Batu.....	91
Figure 4.17	Self-potential contour map from SB1 to SB4 generated by horizontal subsurface flow at Sungai Batu.....	93
Figure 4.18	Contour map shows the flow of water direction generated by horizontal subsurface flow at Sungai Batu.....	94
Figure 4.19	Magnitude of self-potential (SP) at Sungai Batu.....	95
Figure 4.20	2-D resistivity inversion model and self-potential profile for SB1(a) to SB4(d) at Sungai Batu.....	96
Figure 4.21	Grain size distribution curve at 0.5 m depth for SS1 at Sungai Batu.....	97
Figure 4.22	Slice by slice for 3m distance of 2-D resistivity and SP at different depth placing vertical a) 2-D resistivity b) self-potential and c) horizontal at Sungai Batu .....	104
Figure 4.23	2-D resistivity inversion model for LJ1 to LJ3 with x-distance (m), y-elevation (m) at Lojing.....	110
Figure 4.24	Self-potential contour map from LJ1 to LJ7 generated by horizontal subsurface flow at Lojing .....	112
Figure 4.25	3-D wireframe map shows the flow of water direction generated by horizontal subsurface flow at Lojing.....	113
Figure 4.26	Magnitude of self-potential (SP) at Lojing .....	114
Figure 4.27	a) 2-D resistivity inversion model on survey lines and b) self-potential contour map on survey lines for LJ1(a) to LJ7(g) at Lojing .....	115
Figure 4.28	Grain size distribution curve at 0.5 m depth for LS1 at Lojing.....	116
Figure 4.29	Borehole drilling in hot spring source at Lojing .....	119

Figure 4.30	2-D resistivity inversion model for SR1 to SR5 with x-distance (m), y-elevation (m) at Kluang District Southern Peninsular Malaysia .....	123
Figure 4.31	Self-potential contour map from SM1 to SM6 generated by horizontal subsurface flow at Kluang District of Southern Peninsular Malaysia.....	124
Figure 4.32	3-D wireframe map shows the flow of water direction generated by horizontal subsurface flow at Kluang District of Southern Peninsular Malaysia.....	125
Figure 4.33	a) 2-D resistivity inversion model on survey lines SR1 to SR3 and b) self-potential contour map on survey lines for SM1(a) to SM6(f) at Kluang District of Southern Peninsular Malaysia .....	126
Figure 4.34	Characterization for different types of water flow .....	129

## LIST OF SYMBOLS

$C_1$ & $C_2$	Concentration of different solutions
$C_E$	Electro filtration coupling coefficient
$E_C$	Electrochemical potential amplitude
$E_K$	Electro kinetic potential
$I$	Current
$k$	Array geometric factor
$m$	Meter
$M$ & $N$	Current electrodes
$mV$	Millivolt
$r$	Distance
$T$	Temperature
$Y$ & $Z$	Potential electrodes
$\eta$	Dynamic viscosity
$\rho$	Resistivity
$\rho_a$	Apparent resistivity
$\Pi$	Pi
%	Percentage
$\Omega m$	Ohmmeter
$\epsilon$	Dielectric permittivity of pore fluid
$\Delta P$	Pressure difference

## LIST OF ABBREVIATIONS

AC	Alternating current
AG1-AG7	Archaeology gallery survey lines
AS1-AS3	Archaeology auger drill points
BS	British standard
CS	Coarse sand
C <sub>c</sub>	Coefficient of curvature
C <sub>u</sub>	Uniformity coefficient
C <sub>H</sub>	Hazen empirical coefficient
DC	Direct current
ERT	Electrical resistivity tomography
ERI	Electrical resistivity imaging
ER	Electrical resistivity
FS	Fine sand
Gra	Gravel
GSDs	Grain-size distributions
K	Hydraulic conductivity
L	Survey lines
LJ1-LJ7	Lojing survey lines
LS1-LS3	Lojing auger drill points
MS	Medium sand
PH1-PH5	Perpustakaan Hamzah Sendut survey lines
PHS	Perpustakaan Hamzah Sendut
PS1-PS3	Perpustakaan Hamzah Sendut auger drill points
PSD	Particle size distribution
PDP	Pole-dipole
SB1-SB4	Sungai Batu survey lines
SS1-SS3	Sungai Batu auger drill points
SP	Self-potential
SR1-SR5	Southern Peninsular Malaysia survey lines for resistivity
SM1-SM6	Southern Peninsular Malaysia survey lines for SP
VFS	Very fine sand



VUI      Visual user interface

## **LIST OF APPENDICES**

- APPENDIX A PART OF CODING FOR NEW DATA SORTING  
PROCESSING PROGRAM (SORTD)
- APPENDIX B SUMMARY RESULTS OF DRY SOIL SIEVING ANALYSIS  
FOR ALL THE DEPTHS AT ARCHAEOLOGY GALLERY
- APPENDIX C GRAIN SIZE DISTRIBUTION CURVE FOR ALL THE  
DEPTHS AT ARCHAEOLOGY GALLERY
- APPENDIX D SUMMARY RESULTS OF DRY SOIL SIEVING ANALYSIS  
FOR ALL THE DEPTHS AT PHS 2
- APPENDIX E GRAIN SIZE DISTRIBUTION CURVE FOR ALL THE  
DEPTHS AT PHS 2
- APPENDIX F SUMMARY RESULTS OF DRY SOIL SIEVING ANALYSIS  
FOR ALL THE DEPTHS AT SUNGAI BATU
- APPENDIX G GRAIN SIZE DISTRIBUTION CURVE FOR ALL THE  
DEPTHS AT SUNGAI BATU
- APPENDIX H SUMMARY RESULTS OF DRY SOIL SIEVING ANALYSIS  
FOR ALL THE DEPTHS AT LOJING
- APPENDIX I GRAIN SIZE DISTRIBUTION CURVE FOR ALL THE  
DEPTHS AT LOJING

**PENGIMEJAN GEOFIZIK DEKAT PERMUKAAN BAGI PENILAIAN  
ALIRAN AIR TANAH CETEK MENGGUNAKAN KAEDAH  
KEBERINTANGAN ELETRIK DAN SWA-KEUPAYAAN**

**ABSTRAK**

Analisis aliran air di bawah permukaan bumi adalah isu penting untuk kajian hidrogeologi, alam sekitar, geoteknik dan kejuruteraan. Walaubagaimanapun, perhatian yang kurang diberikan mengakibatkan bahaya pada kejuruteraan dan alam sekitar yang serius. Oleh itu, kajian ini diperlukan bagi mengurangkan masalah tersebut. Kajian ini bertujuan untuk mengkaji pengimejan geofizik dekat permukaan bagi aliran air tanah cetek di galeri arkeologi, perpustakaan Hamzah Sendut 2, Sungai Batu, Lojing, dan daerah Kluang selatan semenanjung Malaysia. Bagi mencapai tujuan ini, kaedah keberintangan 2-D, swa-keupayaan, dan geoteknik digunakan. Hasilnya mendedahkan bahawa anomali swa-keupayaan -140 hingga 0 mV berkemungkinan ialah aliran air tanah pengimbuhan (penyusupan) yang dibuktikan oleh penyongsangan keberintangan 2-D dengan nilai keberintangan yang rendah  $<100 \Omega\text{m}$  pada kedalaman  $<5 \text{ m}$  yang terkumpul di Kawasan ini, berkemungkinan menunjukkan adanya kelodak berpasir, tanah liat berpasir, dan pasir dengan korelasi fetapan geologi kawasan kajian. Dari hasil lengkung taburan saiz partikel, jenis tanah dan parameter lain yang dapat mempengaruhi kekonduksian hidraulik ditentukan. Selain itu, lapisan tanah tidak terkonsolidasi dari pasir kasar, pasir sederhana, dan sedimen halus lain meningkatkan aliran air kerana keliangan dan faktor kekonduksian hidraulik. Hasil kekonduksian hidraulik (0.00009 hingga 0.001 m/s) menunjukkan bahawa tanah adalah telap, yang berkaitan dengan magnitud swa-keupayaan adalah panjangnya bersaiz sederhana (0.3 hingga 3.7). Sampel yang digunakan dalam kajian ini adalah keadaan tanah bergred

rendah dengan pekali keseragaman ( $C_U$ ) lebih besar daripada 4. Selebihnya, susunan partikel tanah menunjukkan bahawa agregat tanah itu longgar dan rapuh. Saiz partikel tanah, struktur tanah, dan kandungan kelembapan mempengaruhi keberintangan elektrik, swa-keupayaan, dan kekonduksian hidraulik di kawasan aliran air. Jenis aliran air yang berbeza dicirikan berdasarkan jula skala aktiviti pengimbuhan dan luahan swa-keupayaan; berjulat kecil (-30 hingga 46 mV) pada muka air tanah sederhana (-40 hingga 100 mV) pada sumber mata air panas, dan tinggi (-130 hingga 150 mV) pada air bawah tanah. Ini menunjukkan bahawa perbezaan dalam juhat skala mungkin bervariasi dengan kuantiti/jumlah air dan jenis tanah di setiap kawasan. Profil tanah dalam aliran air bawah tanah yang cetek lebih terdiri dari pasir sederhana, pasir kasar, pasir halus, dan beberapa kerikil untuk sisa tanah granit. Manakala tanah alluvial pinggir lant mempunyai pasir yang lebih sederhana, pasir halus, pasir kasar, dan beberapa kerikil. Oleh itu, hubungan antara kekonduksian hidraulik, swa-keupayaan, keberintangan elektrik, dan jenis tanah memberikan maklumat terperinci mengenai sumber air bawah tanah yang cetek dan arah aliran.

**NEAR SURFACE GEOPHYSICAL IMAGING FOR SHALLOW  
GROUNDWATER FLOW EVALUATION USING ELECTRICAL  
RESISTIVITY AND SELF-POTENTIAL METHODS**

**ABSTRACT**

The analysis of water flow in the earth subsurface is a vital issue to hydrogeology, environmental, geotechnical, and engineering studies. Despite this importance, less attention had been given to it which resulted in serious engineering and environmental hazard. This, therefore, necessitate the present study to mitigate the problem. The research aimed to study the near surface geophysical imaging for shallow groundwater flow in Archaeology gallery, Perpustakaan Hamzah Sendut 2, Sungai Batu, Lojing, and Kluang district Southern Peninsular Malaysia. To achieve this aim, 2-D resistivity, self-potential, and geotechnical methods were employed. The results reveal that anomaly -140 to 0 mV of self-potential is likely to be shallow groundwater flow recharge (infiltration) which established by 2-D resistivity inversion with low resistivity  $<100 \Omega\text{m}$  at depth  $<5 \text{ m}$  that accumulated in the region, which possibly indicate the presence of sandy silt, sandy clay and sand with the correlation of the geological setting of the study areas. From the result of particle size distribution curve, soil types and other parameters that can influence hydraulic conductivity (K) were determined. Furthermore, the soil layers were unconsolidated ranges from coarse sand, medium sand and other finer sediments which enhance water flow due to porosity and hydraulic conductivity factors. The hydraulic conductivity result (0.00009 to 0.001 m/s) shows that the soil is permeable, which relate to self-potential magnitude (0.3 to 3.7) of moderate size length. The samples used in this study were poorly graded soil condition because uniformity coefficient ( $C_U$ ) is greater than 4.

More so, the arrangement of soil particles indicates that the aggregate of the soil is loose and friable. The size of soil particle, soil structure, and moisture content influences electrical resistivity, self-potential, and hydraulic conductivity in the area of water flow. The different type of water flow was characterized based on the scale range of recharging and discharging activity of self-potential; small (-30 to 46 mV) in the water table, moderate (-40 to 100 mV) in hot spring source, and large (-130 to 150 mV) in groundwater. This implies that the differences in the scale range may likely be variation in quantity/amount of water and the soil type in each area. The soil profile in shallow groundwater flow consist of more medium sand, coarse sand, fine sand, and some gravel for residual soils of granite, while coastal alluvial soils consist of more medium sand, fine sand, coarse sand, and some gravel. Therefore, the relationship between hydraulic conductivity, self-potential, electrical resistivity, and soil type gives detailed information on the source of shallow groundwater and flow direction.

# CHAPTER 1

## INTRODUCTION

### 1.1 Background of the study

The assessment of water flow in the earth subsurface is a key issue to hydrogeology, environmental, geotechnical and engineering studies. The flow of water is vital for engineers that planning structure of any kind either above or below the ground. Neglecting the effect of water flow in the soil may be more dangerous and deadly. The filtration of water flowing through a saturated sand bed reported by Henri Darcy (Mizunaga and Tanaka, 2010; Singarimbun et al., 2012; Najafi Alamdarlo et al., 2015, Gao et al., 2018). Water below the land surface occurs in two main zones, the unsaturated zone, and the saturated zone (Telford et al., 1990; Brauchler et al., 2013; Jougnot et al., 2015). Both air and water fill spaces between the cracks in rocks and particle grains in the unsaturated zone (Nwosu et al., 2011; Thompson et al., 2012; Perrone et al., 2014; Voytok et al., 2016), in the unsaturated zone reasonably amount of water may be present, which hold it tight by the forces of capillary that cannot allow pumped from the wells (Demissie et al., 2009; Jardani et al., 2009; Straface et al., 2011; Gokturkler and Balkaya, 2012; Essa and Elhussein, 2017). The saturated zone is filled with water in the voids, in contrast to the unsaturated area (Juanah et al., 2013; Mehane, 2015; Susilo et al., 2017; Tito and Firdaus, 2018). The water table is the surface of the saturated zone and water below the water table in the saturated zone is known as groundwater (Sill, 1983; Linde et al., 2011; Rosas et al., 2014; Mao et al., 2015; Biswas, 2017). The places in which surface water infiltrates into the soil are recharge zones, where groundwater is found and the places in which groundwater seeps or flows into surface water are discharge zones (Shalivahan and Agarwal, 2009; Hasim et al., 2013; Al-Fares, 2014; Shirazi et al., 2015). Just like water on the surface,

groundwater can also flow, and groundwater also flows downhill (Revil et al., 2004; Robert et al., 2011; Gabrielli et al., 2012; Jayeoba and Oladunjoye, 2015). More porous materials will increase the rate of flow, while those of more solid will reduce the rate of flow (Fournier, 1989; Maxwell et al., 2014; Harry et al., 2018; Muhammad, 2019). From the overlying rock, soil, and water, groundwater can also move in response to pressure differences (Graham et al., 2010; Khatri et al., 2011; Grandjean et al., 2011; Idris et al., 2015; Massuel et al., 2017).

There is a need to sort 2-D resistivity and self-potential raw data before interpretation. This step is called the processing step and involves a lot of data sorting. There are problems associated with too many data while focusing on every distance and depth of each data this caused data sorting processing become a tedious task. When one resulted to manual data sorting, mistakes may occur especially when involving hundreds or thousands of data. To trace the mistake may be difficult and time-consuming. Therefore, the idea to minimize the mistakes and time taken for sorting the data manually in an excel file, lead to develop of a new data sorting processing program (SortD) for 2-D resistivity and SP data. The data from the sorting program were used to produce slice by slice imaging which gives information to identify detail view from 2-D resistivity and self-potential imaging. This program can also be used for sorting data in any geophysical methods like induced polarization, seismic, magnetic, and gravity. Data processing is one of the important parts of geophysical methods. The geophysical methods have merits and demerits peculiar for each. To overcome these two or three geophysical methods needed to be combined for a better understanding of shallow groundwater flow. Therefore, the importance of water flow has driven this study to focus on the application of geophysical methods and geotechnical method.



In 2-D resistivity is a fact that electrical potential is spread in the ground surround electrode carrying a current which determines by the electrical resistivities and the spread of the soils and rocks surrounding it, in electrical resistivity survey of the surface (Loke et al., 2014; Majzoub et al., 2017; Abd El Gawad et al., 2017).

Self-Potential (SP) is the natural occurrence of electric fields that originate anywhere in the earth (Skianis, 2012; Emujakporue, 2016; Allegre et al., 2010; Okan, 2015). SP generated by groundwater flows with respect to a solid, and is the only geophysical method directly related to the water transport in the soil (Martínez-Pagán et al., 2010; Moore et al., 2011; Giampaola et al., 2016). Therefore, subsurface information was given using geophysical methods. The usual limitation is lack of sufficient contrast in physical properties, the soil hand auger is used to take the wet soil samples, the soil was washed, and dry in oven, the sieving was done using a collection of British Standard Soil Classification System (BS410/1986) sieve and borehole records in the study areas.

The undisturbed soil samples are taking for physical analysis using soil hand auger for boring to the depths where samples were obtained, and the sieve size analysis was done on the soil samples to get particle size distribution (PSD) and hydraulic conductivity (K).

## **1.2 Problem Statements**

The inadequate knowledge of water flow has resulted in serious engineering and environmental hazard such as loss of life, properties due to flooding and landslide. There are several reports of structures failure in the study areas. Therefore, SP, electrical resistivity and hand auger methods (soil sample) were used for the investigation. In recent years SP method has been increasingly used and the exact

physical processes still unclear. SP method is not definitive; therefore, it should be integrated with other geophysical methods for better interpretation. The problem associated with 2-D resistivity is the vertical view image while self-potential (SP) is the horizontal view image which make it difficult to relate both. Hence, it necessitates harmonizing the image view of both method for better visualisation. The five study areas have different soil type. Then, it will contribute to different permeability. As the water flow is highly dependent on permeability of the soil, it is very crucial to study soil type. Since the study area consists of different soil type which effect resistivity value, but that of self-potential value was unknown. Therefore, to investigate the problem, soil profile of these site will be established, the method used is auger together with electrical resistivity, self-potential, and hydraulic conductivity in shallow groundwater flow.

### **1.3 Objectives**

The research work was carried out in order to have insight into the shallow groundwater flow, to see the relationship between 2-D resistivity, self-potential methods and geotechnical method.

The objectives are as follows:

- (i) To determine the potential of water flow using 2-D resistivity and self-potential methods
- (ii) To evaluate the relationship between hydraulic conductivity (K), self-potential magnitude, and grain size distribution in shallow groundwater flow
- (iii) To establish near surface soil profile for shallow groundwater flow

### **1.4 Significant and Novelty of the study**

The hydraulic conductivity (K) shows that the soil is permeable, which can be relate with self-potential magnitude. The different types of water flow were

characterized based on the activities of the recharge and the discharge scale of self-potential (SP) as lower in water table, moderate in hot spring source, and higher in groundwater in relation to geotechnical analysis. The integration of hydraulic conductivity, self-potential, electrical resistivity, and soil type gives detailed information on the source of shallow groundwater and flow direction.

## **1.5 Thesis layout**

The thesis consists of 5 chapters which are layout as follows:

Chapter 2 provides fundamentals discussion on water flow, groundwater, and the water cycle. This chapter discusses the basic theory of 2-D resistivity, self-potential, and soil hand auger. This chapter also includes some previous research works related to this research to give an overview of water flow, groundwater potential and the methods used, with application of 2-D resistivity, self-potential, and hydraulic conductivity in relation to water flow.

Chapter 3 presents the methodology used in this study with the following, introduction to groundwater movement, flow chart of the methodology, the map of Malaysia showing all the study areas, discussion of all the study areas geology with sedimentary, limestone, granite and other igneous rock, stratified rocks older than granite and alluvium. This chapter also explains how data acquisitions were done using 2-D resistivity and self-potential methods. The newly developed data sorting processing program, the language used C# and the explanation on how the new program works from developing to the usage in detail. SortD program is unique from the existed program due to its sorting ability according to distance specification for slice by slice in view imaging. Soil samples collection using soil hand auger was done in four sites of the study area. Sieving analysis, and grain size distribution (GSDs),

calculation and expression of results, the results were plotted to get grain-size distributions also using an empirical formula Hazen because the soil is saturated and sandy to calculate hydraulic conductivity (K).

Chapter 4 provides all the results of 2-D resistivity, self-potential and grain size distributions curves for five study areas and the new computed program SortD used to process 2-D resistivity data to produce slice by slice in view imaging, and the soil sample was processed using sieve analysis with % passing was plotted against the particle diameter from the particle size distribution, the empirical formula of Hazen due to the soil is saturated and sandy to calculate the hydraulic conductivity (K) and other factors which hydraulic conductivity depends on such as uniformity coefficient ( $C_U$ ), coefficient of curvature ( $C_c$ ). From all the results, the water flow pattern (direction) was located for all the study areas, from the integration of 2-D resistivity and self-potential the negative anomaly of SP is shallow groundwater flow which is established by inversion model of 2-D resistivity. Sorting image help in the trend of contour imaging of 2-D resistivity in slice by slice. Also, the investigation of particle size distributions using the grading curve, the soils are classified into basic soil-type, and the result of hydraulic conductivity was related to the self-potential magnitude. This study has shown the importance of 2-D resistivity, self-potential, hydraulic conductivity, and soil type which gives detailed information on the source of water flow, flow direction, which can strengthen water management also, use in environmental and engineering problems.

Chapter 5 concludes the whole thesis by relating it to the objectives of this study and some recommendations for future research.

## **CHAPTER 2**

### **LITERATURE REVIEW**

#### **2.1 Introduction**

The structure of the soil influenced water flows through it, water and air exchange where connecting pores. Primarily the size of the pores and the relative amount of sand, silt, and clay dictate the flow of water in the soil not only porosity (Jouniaux et al., 2009; Pliakas and Petalas, 2011; Ishaku et al., 2011). Soil texture is the main factor that affects soil structure origination (Bumpus, 2010; Thompson et al., 2012; Massuel et al., 2017). The originates of freshwater that turn into groundwater is sectional recharge from rainfall that infiltrates to the water table along the unsaturated zone, streams water loss and surface water such as wetlands and lakes (Moore et al., 2011; Mao et al., 2015; Novie and Thomas, 2018). Groundwater may gain water (recharge) or lose water to lakes, streams, and wetlands (Ikard et al., 2013; Alakayleh et al., 2018). The interconnected pore spaces in finer-grained sediments smaller than those in sand and gravel, and the hydraulic conductivity (K) of the finer-grained materials is smaller than the hydraulic conductivity (K) of sand and gravel (Jardani et al., 2013; Soueid Ahmed et al., 2016; Hasan et al., 2019). The capability of earth matter to hold water differs from different types of materials. Since the beginning of the earth the water cycle has remained the same, also called the hydrologic cycle (Tadanori et al., 2012; Tebakaria and Kitaa, 2015; Oliveti and Cardarelli, 2017). Eventually, water flowing over the surface or through the ground makes its way into lakes and rivers or is absorbed by trees and plants, where it transpires or evaporates to begin the cycle again (Chapuis, 2012; Emujakporue, 2016) as shown in figure 2.1.

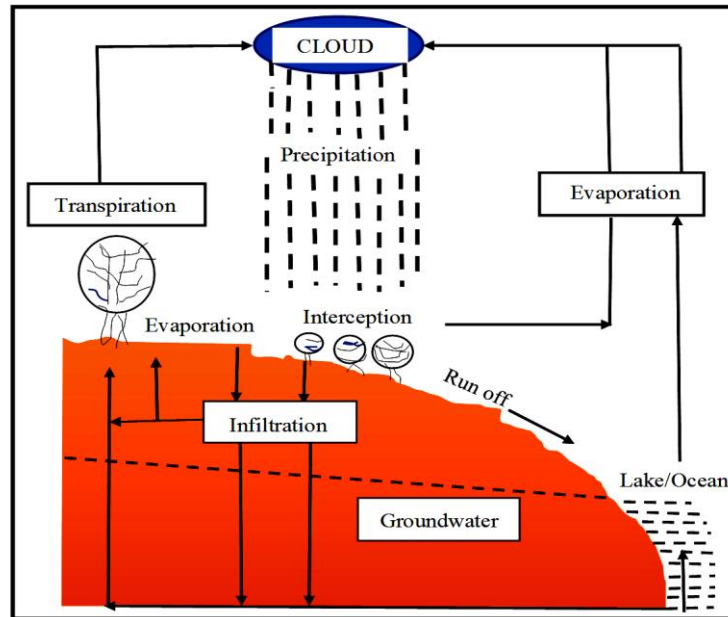


Figure 2.1 Water cycle or hydrological cycle

Water flows in a stream is control by many features such as:

- **Precipitation:** In the watershed, the amount of precipitation that falls as rain or snow is the greatest factor controlling streamflow. Thus, on the watershed, not all precipitation flows out, from precipitation when there is no direct runoff the stream will continually flow (Ghafar et al., 2016; Muhammad, 2019).
- **The land slope:** Water drop on flat land runs off slowly than water drop on steeply sloped land (Gabielli et al., 2012; Voytek et al., 2016).
- **Infiltration:** The infiltration of some water into the soil when the rain falls on the dry ground. In the shallow soil layer, some of the infiltrates water will remain, and move slowly downhill and flow into the stream bank (Skianis et al., 2012; Gao et al., 2018). Recharging the aquifers when some water infiltrates much deeper in the soil (Ikard et al., 2013; Giampaolo et al., 2016). The volume of water that will soak in watershed overtime depends on:

- Soil characteristics: clayey and rocky soils absorb less water at a slower rate than sandy soils. When soils absorb less water more runoff occurs over the land into streams (Grandjean et al., 2011; Oni et al., 2017).

Darcy's law assumes that the flow of a fluid with constant viscosity across a rock is only a function of its pressure difference, and the rock properties (e.g., permeability) remain constant with time. The soil types in Peninsular Malaysia are generally, three main soil groups which are: residual soils of granite, residual soils of sedimentary, and coastal alluvial soils (Hasim et al., 2013; Shaari et al., 2016). Residual soils are formed from the weathering process of rocks. Granitic soils generally contain high sand content with low water content. Alluvial soils are also known as fluvial soils or alluvium. These soils are transported to their present position by rivers and streams (Saleem et al., 2010; Ahmad et al., 2014). A soil is said to be permeable when it allows water through it. There are various factors that affect permeability of soils such as size of soil particle: permeability varies according to size of soil particle. If the soil is coarse grained, permeability is more and fine grained, permeability is low. Shape of the particle: rounded particles will have more permeability than angular shaped, due to specific surface area of angular particles is more compared to rounded particles. Specific surface area of particle also effects the permeability, higher the specific surface area lower will be the permeability. Void ratio: permeability increases with void ratio, but it is not applicable to all types of soils. Soil structure: structure of any two similar soil masses at same void ratio need not be same, it varies according to the level of compaction applied. Degree of saturation: partially saturated soil contains air voids which are formed due to entrapped air or gas released from the percolating fluid or water (Garba et al., 2014; Shaari et al., 2016). This air will block the flow path thereby reduces the permeability; fully saturated soil is more permeable than partially saturated soil.

Water properties: various properties of water or fluid such as unit weight and viscosity also effect the permeability. Temperature also affects the permeability in soils. Adsorbed water is the water layer formed around the soil particle especially in the case of fine-grained soils. Organic matter: presence of organic matter decreases the permeability, due to blockage of voids by the organic matter (Jougnot et al., 2015; Rendana et al., 2019). Some of these factors that affect permeability also affect geophysical analysis.

## **2.2 2-D Resistivity**

The basic principle of 2-D resistivity investigations is to map subsurface resistivity by injecting an electrical current on the surface of the ground (Al-Fares, 2014; Harry et al., 2018). The resistivity measurement on the ground depends on some features like porosity, the content of mineral, water saturation degree in rock and fluid content that may impact values of resistivity (Saad et al., 2012; Loke et al. 2013; Jayeoba and Oladunjoye, 2015; Tan et al., 2015). The soils and rocks resistivity are basically dominated by the number of water pore, different lithology is shown by different resistivity (Wightman et al., 2003; Loke et al., 2014; Hajizadeh and Akhondi, 2016). The groundwater-surface granular soils, coarse, a sudden change in resistivity and water saturation usually notice (Abidin et al., 2015; Syukri and Saad, 2017). Inhomogeneous soil the measurement between two points on the Earth's surface of electrical resistivity depends on the sensitivity of the ground known as apparent resistivity (Pandey et al., 2015; Azhar et al., 2016). To calculate apparent resistivity the potential difference for the interpretation is used as indicated in figure 2.2. If the electrode carries a current  $I$ , measured in amperes, the potential at any point in the medium or on the boundary is given by equation 2.1:



$$V = \rho \frac{I}{2\pi r} \quad 2.1$$

Where,

$V$  = potential,  $\rho$  = resistivity of the medium,  $r$  = distance from the electrode

The potential at  $Y$  can be found using equation 2.2,

$$V_1 = \frac{\rho a I}{2\pi} \left( \frac{1}{MY} - \frac{1}{YN} \right) \quad 2.2$$

The potential at  $Z$  can be find using equation 2.3,

$$V_2 = \frac{\rho a I}{2\pi} \left( \frac{1}{MZ} - \frac{1}{ZN} \right) \quad 2.3$$

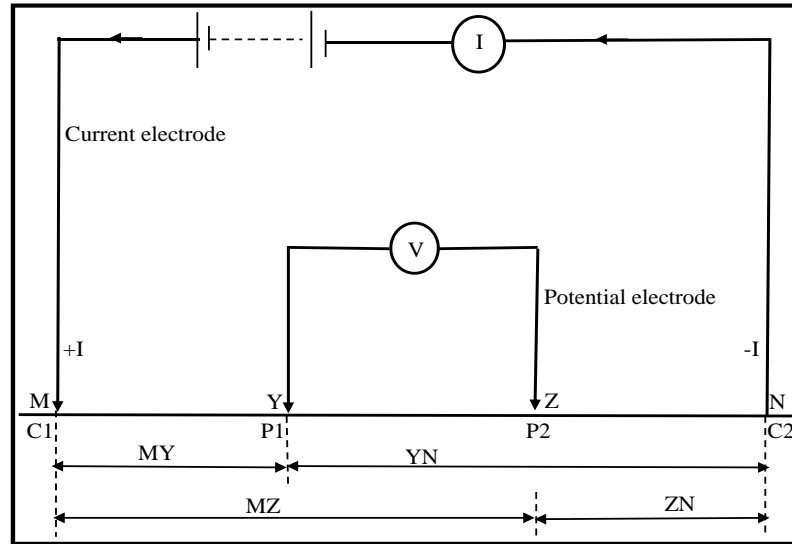


Figure 2.2 Basic concept of electrical resistivity measurement

Following the previous equations, the potential difference  $V$  may be written as

$$\Delta V = \frac{\rho a I}{2\pi} \left\{ \left( \frac{1}{MY} - \frac{1}{YN} \right) - \left( \frac{1}{MZ} - \frac{1}{ZN} \right) \right\} \quad 2.4$$

The parameter inside the brackets is a function of various electrode spacings and denoted by  $1/k$ , which is written in equation 2.5:

$$V = \frac{\rho I}{2\pi K} \quad 2.5$$

Where  $k$  = array geometric factor.

Equation 2.5 can be rewritten as equation 2.6:

$$\rho = 2\pi k \frac{V}{I} \quad 2.6$$

The resistivity of a medium can be found from measured values of  $V$ ,  $I$ , and  $k$ , the geometric factor (Ghafar et al., 2016; Peter et al., 2016; Mohamed et al. 2016).  $k$  is a function only of the geometry of the electrode arrangement as shown in equation 2.6.

### 2.3 Self-Potential Method (SP)

A self-potential method is established when electrochemical reactions in the subsurface produce the surface measurement of natural potentials, injection of electric currents is not needed into the ground as in the case of resistivity and induced polarization (IP) methods (Roudsari and Beitollahi, 2015; Giampaola et al., 2016). SP method is passive, i.e. between any two points on the ground surface differences in natural ground potentials are measured, the measured potentials from millivolt (mV) to Volt and in the interpretation of SP anomalies the +ve or -ve sign of the potential are vital feature (Linde et al., 2011; Okan and Osazuwa, 2015). When water reacts as an electrolyte and as a different minerals' solvent, the potentials are generated by water flow, which is the common factor responsible for SP (Singarimbun et al., 2012; Muztaza et al., 2018). There are two types of array in study self-potential which are gradient and fixed base array. There are some types of SP such as (a) mineral/mineralization potential (b) Thermoelectric potential (c) Electrochemical potential: If the concentration of the electrolyte in the ground varies locally, as a result of change in anions and cations mobilities the potential differences are set up in solutions of different concentrations known as diffusion potentials (Doussan et al., 2002; Revil & Leroy, 2004; Chukwu, 2013), the electrochemical potential amplitude ( $E_c$ ) is given by equation 2.7

$$E_c = -70.7 \frac{T+273}{273} \ln \frac{C_1}{C_2} \quad 2.7$$

Where  $C_1$  and  $C_2$  are concentration of different solutions with the same temperature,  $T$  ( $^{\circ}\text{C}$ ) is temperature.

(d) Electrokinetic potential: Fluid (electrolyte) Flow in a medium porous generates potentials within the flow path known as electrofiltration, streaming potentials and the fluid ions and the walls of the capillary/ porous medium caused by electrokinetic coupling between them (Jardani et al., 2007; El-Sayed et al., 2016).  $E_k$  is electrokinetic potential generated is given by equation 2.8

$$E_k = \frac{\epsilon\rho C_E \Delta P}{4\pi\eta} \quad 2.8$$

Where,  $\epsilon$  = Dielectric permittivity of pore fluid;  $\rho$  = Electrical resistivity of pore fluid;  $C_E$  = Electrofiltration coupling coefficient;  $\Delta P$  = Pressure difference;  $\eta$  = Dynamic viscosity of pore fluid.

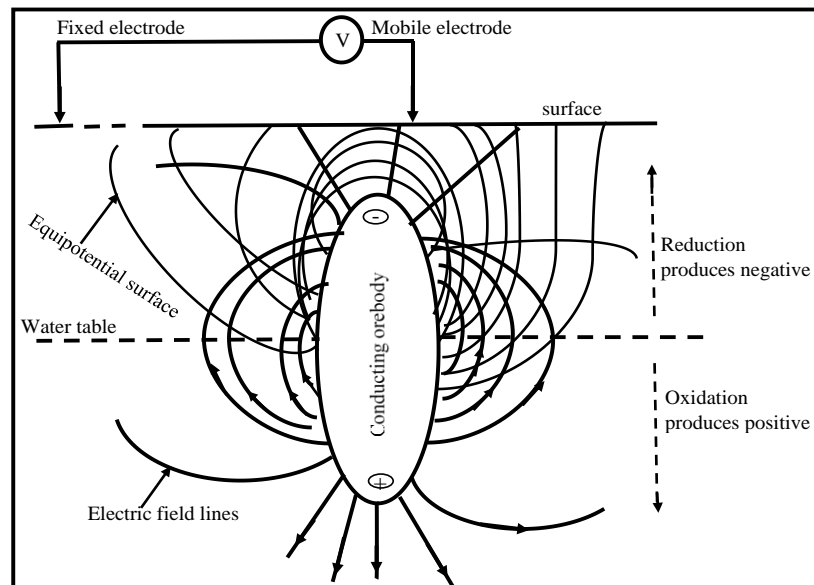


Figure 2.3 Simplified model of the origin of self-potential anomaly of an orebody. The operation based on differences in oxidation potential above and below the water table

## 2.4 Soil Hand Auger

Auger has a wide variety of heads and can select the most suitable auger for specific soil types. Extension pieces come in various lengths, cross handles, and core

cutters. A soil hand auger is the best tool for sampling collection. A hole is bored into the soil with the hand auger to a certain depth where the core cutter is used to take the soil samples. In the laboratory, the core with the soil was weighed ( $m_c$ ). A clean receiving pan was weighed and recorded ( $m_1$ ), and wet sample (saturated soil) was washed and added into the receiving pan and weighed and recorded ( $m_2$ ). To get the weight of the moist sample ( $m_w = m_2 - m_1$ ). The moist sample was then transferred into an oven set at  $105^{\circ}\text{C} \pm 5^{\circ}\text{C}$  and left for 3-4 hours after which it is allowed to cool, and the weight taken ( $m_s$ ) and proceed for sieving analysis.

#### **2.4.1 Sieve Analysis and Grain-Size Distributions (GSDs)**

Sieving was done mechanically, the known quantity of dry soil by a set of British Standard Soil Classification System (BS410/1986) sieve with mesh sizes (No ¼", 4, 5, 6, 7, 8, 10, 12, 14, 16, 18, 20, 25, 30, 35, 40, 45, 50, 60, 70, 80, 100, 120, 140, 170, 200, 230 corresponding to equivalent diameter 6.30, 4.75, 4.00, 3.35, 2.80, 2.36, 2.00, 1.70, 1.40, 1.18, 1.00, 0.85, 0.71, 0.60, 0.50, 0.43, 0.36, 0.30, 0.25, 0.21, 0.18, 0.15, 0.13, 0.11, 0.09, 0.075, 0.063 mm respectively. The soil sample is then sieved. The soil retained on each sieve is weighed and the percentage of the entire material that is passing through each sieve can enter a grain size diagram. The hydrogeological conductivity can be affected by the grain size distribution of the soil. A sorted soil having bigger grains will have hydraulic conductivity high. The K will be low when more multi-graded soil and grain sizes are present in sediment (Fetter, 2001; BCE, 2017). Due to the smaller grains filled up the void between larger grains.

The hydraulic conductivity (K) is the capacity measurement of the soil to transmit water and in studying the subsurface flow and transport problems. The hydraulic conductivity of unconsolidated geologic material is relating to empirical formulas from sieve analysis and obtained grain size distribution. From grain size

distribution curve  $K$  is estimated:  $D_{10}$ , the grain diameter for which 10% of the sample is finer (90% is coarser), and  $D_{60}$ , the grain diameter for which 60% of the sample is finer (40% is coarser) (Fetter, 2001; Salarashayeri and Siosemarde, 2012). The effective diameter of the sample is  $D_{10}$ , the ratio  $C_U = D_{60}/D_{10}$  is defined as uniformity coefficient and  $C_C = D_{30}^2 / D_{60} \times D_{10}$  is defined as curvature coefficient. The  $K$  value of the saturated soil is then considered from the standard formula given by Hazen  $K = C_H (D_{10})^2$  Salarashayeri & Siosemarde (2012) from a grain size distribution curve.

## **2.5 Previous Work**

A number of works have been done on subsurface groundwater flow using self-potential method and hydraulic conductivity shown that complex conductivity spectra are sensitive to some textural parameters controlling permeability such as the main pore-throat size (Straface and Chidichimo, 2010; Lopez et al., 2015). Also, evaluation of empirical formulae for the determination of hydraulic conductivity based on grain-size distribution, or the surface area per pore volume ratio (Salarashayeri and Siosemarde, 2012; Paradis et al., 2015; Van Ginke and Olsthoorn, 2019) and 2-D resistivity and self-potential to determine the groundwater flow (Nwosu et al., 2011; Abidin et al., 2015; Susilo et al., 2017). Less recognition had been given to groundwater flow despite its importance, which resulted in serious engineering and environmental hazard. Therefore, the reviews of relevant literature, of 2-D resistivity, self-potential and hydraulic conductivity related to shallow groundwater flow in granitic rock/coarse grain were done. Table 2.1 show the summary of previous literature reviews.

### **2.5.1 Granitic/coastal grain**

As reported by Gernez et al. (2019) developed a new methodology based on an innovative anisotropic ERT modeling tool and the relationship between  $K$ - and  $\rho$ -

anisotropies through an *in-situ* survey. Gernez et al., suggested a strong link with the collocated *K*-anisotropic characterization: even though the setup used does not allow a direct proportionality relation, the proposed geophysical method is able to provide proxy of the *in-situ* hydraulic anisotropy. Integrating with other geophysical method was not done which can give better understanding in order to produce more reliable forecasts.

As study by Chen et al. (2018) developed a method to estimate the spatial distribution of *K* for a composite fan delta by integrating dense VES measurements with some pumping test data. data classification, linear regression, and kriging interpolation. The data classification was conducted using a physical-based zonation method. The *K* and formation factor (*F*) data pairs were classified into several groups. Linear regression was used to develop *K-F* mapping for each group. By integrating highly dense electrical resistivity measurements and some pumping test data, the developed approach makes spatial *K* estimation for a regional groundwater system more efficient and economical than only relying on traditional pumping tests. The estimated errors were between 7 m/day and 58 m/day, and the correlation coefficient of each data group was >0.8. Based on these regression equations and ordinary kriging method, the detailed *K* spatial distribution of the study area was derived. Other geophysical method should be integrated for better understanding to produce more reliable result.

Based on Alakayleh et al. (2018) which develop a scalable framework for modeling the changes in hydraulic conductivity values due to the presence of fine material. investigated the performance of a scalable model that used for predicting the changes in the hydraulic conductivity value of coarse and fine porous media mixtures due to the presence of different amounts of fines. Several laboratory experiments that represented the percentage of fines ranging from 0 to 30 were conducted using

simulated coarse-fine and fine-coarse synthetic porous media mixtures. The value of the hydraulic conductivity of the coarse porous media decreased as the percent fine increased in the mixture. There was a significant reduction in hydraulic conductivity when started to add fine material to the coarse material; however, the reductions became less significant when the percentage of fine exceeded about 15%. Typically, the overall hydraulic conductivity value of the mixture was almost close to the hydraulic conductivity of the fine particles when the percent of the fine was above 30%. The integration of geophysical methods was not done which can give better understanding for more reliable forecasts.

According to Soueid Ahmed et al. (2016) perform a 3D synthetic confined aquifer and the adjoint state method to compute the sensitivities of the hydraulic parameters to the hydraulic head and self-potential data in both steady-state and transient conditions. Soueid Ahmed et al., compared the results obtained from the hydraulic tomography alone and from the combination of the self-potential method and the hydraulic tomography during a series of transient pumping/injection tests. The petrophysical formulation of the material properties in the forward modeling of the self-potential field is used. Therefore, electrical resistivity and the magnitude of self-potential were not jointly used and consider.

Shaari et al., (2016) present an idea about varying infiltration rates with varying soil types and the area is mainly comprised of Quarternary alluvium having fluvial and marine origin which is constituted of mainly sand, gravel, silt and clay underlain by granite and metasedimentary rocks. The soil properties like texture, structure, water content, temperature and other factors like vegetation types and cover, and rainfall intensity play a significant role in controlling infiltration rate. Generally, coarse grained soils having large pore spaces with stable structure allows water from rainfall to enter

unimpeded throughout a rainfall event. It has been identified that most of the soil in the study area exhibit low permeability comprising about 70% of the soil. A few patches show moderate to high permeability comprising 15%, whereas 5% of the soil is constituted of very high permeability. Any sizeable reduction in the infiltration of water will subsequently increase the chances of flood occurrences. This situation will become a disaster when the runoff is high and the soil's ability to infiltrate the water is low. Geophysical methods should be integrated for better understanding.

Based on Malama (2014) research to develop a semi-analytical solution of the self-potential field associated with transient hydraulic response of an unconfined aquifer to continuous constant rate pumping. Malama et al., assumed that flow occurs without leakage from the unit below a transverse anisotropic aquifer and neglect flow in the unsaturated zone by treating the water-table as a moving material boundary. This analytical solution is tested using data recorded at the Boise Hydrogeophysical Research Site (BHRS) to determine aquifer hydraulic conductivity, specific storage and specific yield, and is shown to fit measured data well and yield parameter values that compare well to published results for the research site. From this result, the magnitude of self-potential and electrical resistivity was not put into consideration.

According to Ozaki et al. (2014) a two-dimensional inversion code for analyzing the water head distribution from the SP profile was developed. Also developed a two-dimensional inversion code for analyzing the permeability structure from the distribution of the water head. Ozaki et al., combined these two inversion codes and developed an inversion code for analyzing the permeability structure from a SP profile. The inversion is applied to synthetic data affected by subsurface permeability anomalies. The results indicate that the SP inversion can produce a more accurate image of the permeability structure when the SP signal caused by the permeability anomaly is



large. Therefore, the electrical resistivity and magnitude of self-potential were not investigated attentively.

The study of Soueid Ahmed et al. (2014) developed a formula to infer directly from the joint inversion of self-potential and head data the hydraulic conductivity field of a heterogeneous aquifer in three-dimensional. Soueid Ahmed et al., based the approach on the adjoint-state method to compute the sensitivity matrix of the self-potential observations to the hydraulic conductivity. Also, to underline the strengths and weaknesses of the self-potential method for determining K-fields during pumping tests. In this research, information on magnitude of self-potential and electrical resistivity were missing.

As reported by Straface et al. (2011) the combine sedimentological, hydraulic, and geophysical information to characterize the three-dimensional distribution of transport properties of a heterogeneous aquifer. Focused were on the joint inversion of hydraulic head and self-potential measurements collected during an extensive experimental campaign performed at the Boise Hydrogeophysical Research Site (BHRS), Boise, Idaho, and involving a series of dipole tests. The procedure adopted allowed a reconstruction of the heterogeneity of the site with a level of details, and a multiple indicator Kriging to estimate the probability of occurrence of each geo-material. Therefore, electrical resistivity and the magnitude of self-potential were not jointly used and consider in this research.

Base on the study of Azza (2010) to evaluates bio-ecological drainage system (BIOECODSTM) eco-friendly efficiency using streaming potential (SP) signals in Malaysia and the SP result shows the positive anomalies in order of 4 mV to 35 mV indicate water flow in the subsurface and the BIOECODSTM component, swale was directly related. The moderate SP voltages value and polarity show depression

landscapes over the slightly elevated ground and the lower and occasionally negative polarity signatures in many places for dry spots. inconsistency and strongly depend on the landscape, permeability, porosity, and moisture of soil formation, water saturation, and the climatic daily variation affect the SP values of the studied area. Integration of the physical parameters was not observed, which can give better understanding of the seepage when applied with geophysical methods.

The study of Gallas et al. (2011) evaluate contamination using self-potential, resistivity and induced polarization. The direction of flow was characterized using the self-potential technique. The most contaminated area by the leakage have low resistivity, non-contaminated areas by the leakage have high resistivity. The response of the parameter of IP is like display by the resistivity result. The changeability of lower values is associated with higher contamination. However, in the phreatic electrolyte higher ion concentration is associated with contaminated areas of lower resistivity, which favors electrical ionic conduction. The SP method reveals the direction of flow from electrical potential low to high. The information regarding the groundwater flow is not complete without physical parameters.

As reported by Minsley et al. (2011) used direct current resistivity and self-potential surveys to carry out hydrogeophysical investigations with the purpose of assessing seepage patterns and provide information about subsurface geologic structures that may control subsurface flow and seepage. The increase in porosity and permeability in the areas that cover with sediments or weathered granite flow occurs, rather than competent bedrock areas. The sediment is a factor that contributes to the seepage on the dam northwest as indicate in resistivity result. They concluded that most likely significant controlling factors for the observed seepage are the reservoir head upstream, subsurface granite, and surface topography downstream. The physical

parameters enhance the understanding of subsurface flow/seepage, which was not considered in this study.

In Moore et al. (2011) electrical resistivity and self-potential surveys applied for seepage. The contoured map of SP data which exhibits values from (-40 mV to 170 mV). Around the crest, the SP negative zone is found, and both the upstream and downstream the SP positive are found. Groundwater inflow from adjacent hillslopes due to positive SP. The combined analyses suggested that seepage erosion is not affected, and as observed by the sediment the downstream is likely outflow events of the last remnant. The details regarding the seepage is not complete without physical parameters.

Linde et al. (2011) reported the sensitivity of self-potentials (SP) to water fluxes and saturated and unsaturated gradients concentration of geological media in north-eastern Switzerland. The SP sources are situated in soil cover rather than gravel. The time-series of wavelet analyses indicate a strong but on SP signals record the variations in water content, rainfall intensity and water table impact non-linear. The vadose zone has a very strong influence on soil properties distribution when increases precipitation and water table elevation, response with respect to SP modeling, vadose zone thickness or hydraulic head and SP signals semi-empiric relationships were proposed between them, are less complicated than the responses of SP on the gravel bar observed. Given information regarding the subsurface structure and seepage regime is not complete without physical parameters.

According to Thompson et al. (2012) the integration of electrical resistivity (ER), lake-level measurements and self-potential (SP) to study the hydrological processes and structure. The residual streaming-potential reveal from -30 to 70 mV in various non-glacial settings with water seepage through the earth is steady. Their

findings confirm base on tracer tests, geological mapping and observed lake-level which is steady with the hydraulic efficient link in the survey and have notable implications in the investigation. The areas of degradation and potential weakness were caused by flow and subsurface water saturation. Integration of the physical parameters was not observed, which can give better interpretation of the seepage when applied with geophysical methods.

Voytek et al. (2016) reveal that the ERT inversions delineate zones in the subsurface which check flow tracks and SP reacted to groundwater flow on the hillslope. The hilly areas are always associated with slope failure and landslides. The topography, climate, geology, and land use are few prevalence factors of failures. Some countries have different rainfall patterns but similar soils, or some with different land use but similar rainfall. The potential causes of unstable areas are the use of steep natural slopes for housing and road. The physical parameters enhance the understanding of subsurface flow, which was not examined in this study.

As stated by Giampaolo et al. (2016) the time-lapse on salty water leakages by self-potential (SP), hydrogeophysical inversion approach is used to estimate the porous material from diffusion and dispersivity parameters. The negative self-potential anomalies are generated from the movement of the plume salt and there is a sharp reduction in SP measurement with electrical potential negative values of  $-78.99 \pm 3.24$  mV,  $-54.52 \pm 2.28$  mV, and  $-24.12 \pm 1.21$  mV decrease with tracer volume increasing. Self-potential is applied to find diffusion and longitudinal dispersivity by first using Planck-Henderson equation to convert mV into salt concentration values ( $\text{gL}^{-1}$ ) and using the equations implemented in the multiphysics environment COMSOL to calculate the transport parameters, therefore, to spot contaminants at very low

concentrations self-potential can be use. The information regarding the groundwater flow is not complete without physical parameters.

Emujakporue (2016) applied the self-potential method to explore the subsurface in a dumpsite and a neutral environment in Abuja campus, University of Port Harcourt, Nigeria in order to determine the contamination in the lateral extent at an open solid waste disposal site. Emujakporue carried out self-potential measurement at a dumpsite with values range from -7.0 to 2.5 mV and 0. 1 to 9.5 mV in the neutral site. The self-potential maps from the two sites show that the chemical and the subsurface physical properties are not the same. More positive ions were found in the neutral site than the contaminated dumpsite. The biodegradation of the materials in the dumpsite has led to the production of leachate while migrating into the groundwater thereby modifying its physical and chemical properties. The physical parameters enhance the knowledge of subsurface flow, which was not examined in this study.

According to Muztaza et al. (2018) use the 2-D resistivity and self-potential approaches to locate water flow in Malaysia, from their result the 2-D resistivity shows a saturated zone with resistivity value  $< 40 \Omega\text{m}$  (low), consist of sandy silt. The self-potential anomalies range from -42 mV to -8 mV which is used to determine the flow of water directions in the subsurface from north-east high value to the south low value. The combination of physical parameters was not observed which give better interpretation of water flow.

Table 2.1 Summary of the previous works

<b>Authors</b>	<b>Method</b>	<b>Significance</b>	<b>Research gap</b>
Soueid Ahmed et al. (2014 & 2016)	SP, hydraulic head, and electrical resistivity	Use the geostatistical quasi-linear algorithm framework of Kitanidis to solve the inverse problem.	The magnitude of self-potential and electrical resistivity was not put into consideration
Malama (2014); Ozaki et al., (2014) Straface et al., (2010)	SP and hydraulic parameters	Laplace and Hankel's transform are used to solve the coupled flow and electrokinetic problem.	
Gernez et al. (2019); Alakayleh et al. (2018); Chen et al. (2018); Shaari et al. (2016)	Hydraulic conductivity and VES	Electrical resistivity and hydraulic conductivity values of fine- and coarse-grained mixtures	The magnitude of self-potential was not put into consideration
Gallas et al. (2011); Emujakporue (2016); Giampaolo et al. (2016)	SP, electrical resistivity, and IP	To determine the area affected by the pollutants/contaminants.	Integration of the physical parameter was not observed, which can give better interpretation of the seepage when applied with geophysical methods
Azza 2010; Minsley et al. (2011); Linde et al. (2011); Thompson et al. (2012); Voytek et al. (2016)	SP and electrical resistivity	Assessing seepage patterns and provide information about subsurface geologic structures that may control flow seepage.	
Moore et al. (2017); Muztaza et al. (2018)	SP and electrical resistivity	Investigate underground water sources and its movement.	

## 2.6 Chapter summary

This chapter discusses the introduction of water flow, groundwater and water cycle in detail and Darcy law, soil types and factors affecting permeability of soil. Also, the basic principle of electrical resistivity and self-potential, the working principle of soil hand auger, Sieve Analysis, and grain size distributions (GSDs). The importance of hydraulic conductivity in water flow. Some of the review of relevant literature of 2-D resistivity, self-potential related to water movement, and hydraulic conductivity were cited. Soueid Ahmed et al., 2016 and 2014 using the quasi-linear geostatistical